Electron capture by metastable projectiles on He and Ne

J. Newcomb, T. R. Dillingham, James Hall, S. L. Varghese,* Philip L. Pepmiller,† and Patrick Richard
Department of Physics, Kansas State University, Manhattan, Kansas 66506
(Received 21 July 1983)

Electron capture to $n \geq 2$ levels of F^{7+} $(1s\,2s)\,^3S$ projectiles lead to three-electron ions with an energetically allowed K-Auger decay channel. We have measured the F K-Auger emission spectra for collisions with thin gas targets of He and Ne with sufficiently high resolution to distinguish capture to several of the low-lying n values. The K-Auger production cross sections are reported as a function of the n level into which the electron is captured. The n-level dependence is measured for projectile energies of 6, 9, 12, and 15 MeV and is compared to the Oppenheimer-Brinkman-Kramers OBK model for charge transfer and to a $1/n^3$ function. The measured K-Auger electron-production cross sections closely follow the $1/n^3$ function which differs from the predicted OBK n dependence, even though the cross sections for the higher n levels agree with the predicted OBK energy dependence. The effects of cascading upon the calculated n dependence are also studied.

I. INTRODUCTION

In recent years Auger-electron emission has been used to study inner-shell vacancy production[1–3] in ion-atom collisions but, until very recently, has not been widely used to study electron capture. Electron capture, in particular electron capture to excited states of highly ionized atoms, has been, and continues to be, of considerable importance to the studies of plasma energy-loss processes and diagnostics in current fusion-energy programs. The amount of attention that electron capture has accordingly received has been great.[4–7]

The main purpose of the present work has been to further the study of electron capture to excited states of highly ionized atoms in ion-atom collisions utilizing K-Auger electron-emission measurement techniques. Previous investigations of electron capture to excited states have been, for the most part, limited to x-ray and vacuum ultraviolet (vuv) measurement techniques.[6–10] A recently developed technique for studying electron capture to excited states is energy-gain spectroscopy using low-velocity ions.[11–13]

Recent high-resolution x-ray studies at Kansas State University have concentrated on the fluorine-projectile K x rays of the $F^{q+}+He$ and $F^{q+}+Ne$ $(q=2-9)$ collisional systems,[4,5,14,15] while K-Auger studies of these systems have been concerned with the target, rather than the projectile, as the emitter.[2,16] The present work is therefore concerned with the fluorine-projectile K-Auger electron emission of the above-mentioned collisional systems.

The advantages in using K-Auger electron-emission techniques instead of high-resolution x-ray techniques to study the system in question are twofold. One is a matter of detection efficiency. The efficiency of channel-electron multipliers (CEM's) used to detect emitted electrons is known to be about 90% for electrons with an energy of about 1 keV and to vary not significantly with electron energy.[17,18] On the other hand, the crystals used in high-resolution crystal spectrometers have a very low reflectivity. Thus photons with energies in the 1-keV range are severely attenuated (by 3 to 5 orders of magnitude) and, furthermore, the attenuation is highly dependent upon the x-ray energy. The other advantage is the fact that the multiplet fluorescence yields for fluorine are, for the most part, less than 30% and on the average less than 2% (Ref. 19) for the lower charge states indicating that K-Auger decay of the excited states is much more probable than the K x-ray decay of these states. K-Auger measurements are thus much less sensitive to the fluorescence yields.

II. EXPERIMENTAL TECHNIQUES

The experiment was performed in the James R. Macdonald Laboratory at Kansas State University using an EN tandem Van de Graaff accelerator. Fluorine ions of various charges $(q=2-8)$ and with energies of 6, 9, 12, and 15 MeV were used to bombard thin target gases of helium or neon. The resulting fluorine-projectile K-Auger electrons were energy analyzed utilizing an electrostatic cylindrical-mirror analyzer.[16,20]

The resolution of a cylindrical-mirror analyzer has been described in detail in a paper by Risley.[21] The base-width resolution of such an analyzer is expressed in terms of the physical parameters of the analyzer and, for 1-keV electrons, was calculated to be ~ 5.0 eV. Line broadening for the cyclindrical-mirror analyzer involved in the present work (caused by the spread in the scattering angle of the projectiles and by the analyzer having a finite acceptance angle)[1] was calculated to be $9-15$ eV in the rest frame of the emitter for an observed electron energy of 1 keV.[22] The base-width resolution observed in the present work was about $10-15$ eV in the rest frame of the emitter indicating that line-broadening effects were the limiting factor for the resolution of the analyzer.[22]

The criterion used to guarantee predominantly single-collision events was linearity of the projectile K-Auger yield as a function of target-gas pressure. Linearity tests were performed for both gas targets and each projectile charge state. For each projectile charge state, linearity was preserved up to at least 10 mTorr. Running pressures were accordingly kept below 10 mTorr ($\sim 7-8$ mTorr).

III. DATA ANALYSIS

The K-Auger production cross sections were calculated using the equation

$$\sigma_A = C\left[\frac{q}{SP}\right]\sum_i \left[\frac{Y}{Q}\right]_i \left[\frac{I'}{I}\right]_i \frac{1}{E_i}\ , \tag{3.1}$$

where C is a normalization constant, q is the charge state of the incident projectile, S is the full-scale reading of the current integrator, P is the pressure of the target gas measured at the gas cell in mTorr, i is the channel number, $(Y/Q)_i$ is the measured electron intensity per incident ion for channel i after background subtraction, and E_i is the laboratory electron energy for channel i. In obtaining Eq. (3.1), it is assumed that the projectiles do not change charge state in the apparatus and that the Auger electrons are emitted isotropically in the emitter frame.[1]

For projectile K-Auger electrons (i.e., electrons emitted from moving ions), the assumption that the Auger electrons are emitted isotropically has validity only in the projectiles' rest frame. Therefore, if the main concern is with projectile K-Auger electrons, a conversion from laboratory-frame intensity per steradian for each channel i is necessary. The conversion factor, expressed as $(I'/I)_i$ in Eq. (3.1), can be obtained by a simple analysis based on $Id\Omega = I'd\Omega'$ (N.B. primed variables here, and throughout this paper, represent projectile rest-frame variables) and is found to be the following:[1,16]

$$\frac{I'}{I} = \frac{E'}{E}\left[1 - \left[\frac{t}{E'}\right]\sin^2\theta\right]^{1/2}\ , \tag{3.2}$$

where E' is the projectile rest-frame energy of the electron, E is the laboratory energy of the electron, and θ is the laboratory observation angle (42° in the present work).[16] The reduced energy t is defined as

$$t = \frac{m_e}{m_p}E_p \approx \frac{548.6T(\text{MeV})}{A(\text{amu})}\ , \tag{3.3}$$

where m_e is the mass of the electron, m_p is the mass of the projectile, and E_p is the incident kinetic energy of the projectile. The reduced energy can also be approximated in terms of T, the energy of the projectile in MeV, and A, the mass of the projectile in amu.

In order to evaluate Eq. (3.2), the conversion from laboratory energy of the electron to projectile rest-frame energy of the electron is needed. The conversion is given by[1,16]

$$E' = E + t - 2(Et)^{1/2}\cos\theta\cos\beta\ , \tag{3.4}$$

where β is the scattering angle of the projectile. The projectile scattering angle is assumed to be very small and can be set equal to zero for practical purposes. The normalization constant C in Eq. (3.1) was determined for this paper from the Auger yield for 6-MeV $F^{2+}+Ne$ using $\sigma_A = 1.409\times10^{-18}$ cm^2.[23]

IV. DISCUSSION

Fluorine ions with an initial charge state of $q=7$ can be created by passing F^{3+} or F^{4+} ions through a thin ($\sim 10\ \mu g/cm^2$) carbon post-stripping foil. The distribution of charge states thus formed includes the two-electron ion F^{7+}. Not only is a charge-state distribution produced, but, for any given single charge state, many different excited states are also formed. In most cases, these excited states decay to the ground state very rapidly but, for the two-electron ions, a few of these excited states have relatively long lifetimes (see Table I).[24] The times of flight for F^{7+} ions from the post-stripping foil to the gas cell for this experiment are on the order of 1 μsec for the incident energies of F^{7+} ions studied. As can be seen from Table I, only two F^{7+} excited states, the $(1s\,2s)\,^3S$ and $(1s\,2s)\,^1S$ states, have lifetimes comparable to or greater than the time of flight ($\sim 1\mu$sec). Using these values, it can be shown that approximately 99% of the F^{7+} $(1s\,2s)\,^3S$ metastable state created at the post-stripping foil reaches

TABLE I. Lifetimes for the excited states of F^{7+}.

State	Lifetime[a] (μsec)
$(1s\,2s)\,^3S_1$	3.27×10^{2}
$(1s\,2s)\,^1S_0$	1.98×10^{-1}
$(1s\,2p)\,^3P_2$	1.04×10^{-2}
$(1s\,2p)\,^3P_0$	1.10×10^{-2}
$(1s\,2p)\,^3P_1$	5.2×10^{-4}
$(1s\,2p)\,^1P_1$	1.79×10^{-7}

[a]Taken from Ref. 24.

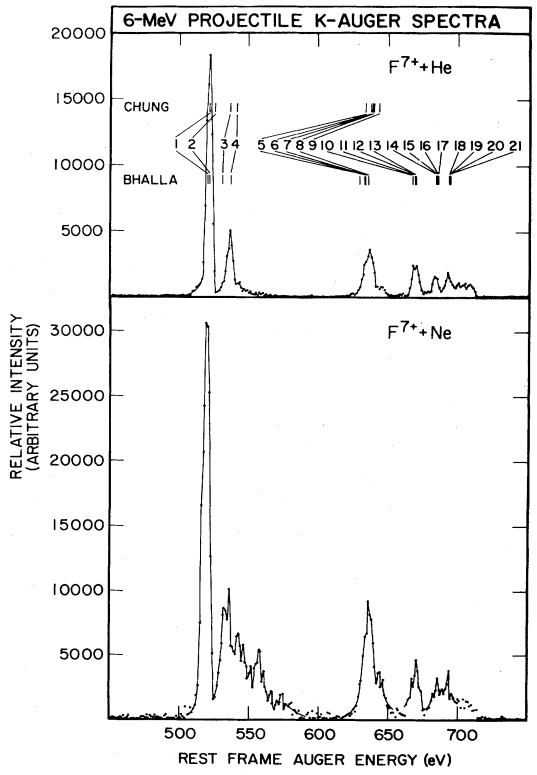

FIG. 1. 6-MeV fluorine-projectile K-Auger spectra for $F^{7+}+He$ and $F^{7+}+Ne$ compared to Auger-energy calculations for $1s\,2snl$ three-electron configurations (see Table II).

TABLE II. Three-electron spectra of fluorine.

	Theory[a] (eV)	Theory[b] (eV)	Experiment (eV)	Experimental error (eV)	Label
$1s\,2s^2(^2S)$	521.6	525.4			1
			521.0	-1.1 $+1.3$	
$1s\,2s\,2p(^4P)$	525.3	525.7			2
$1s\,2s\,2p(^2P_-)$	535.9	535.9	535.9	-1.4 $+1.9$	3
$1s\,2s\,2p(^2P_+)$	541.1	541.7			4
$1s\,2s\,3s(^4S)$	633.3	633.7			5
$1s\,2s\,3s(^2S_-)$	636.6	637.5	635.1	-0.8 $+0.9$	6
$1s\,2s\,3p(^4P)$	637.8	638.0			7
$1s\,2s\,3p(^2P_-)$	638.3	639.4			8
$1s\,2s\,3d(^2D_-)$	642.5		642.9	-2.9 $+2.1$	9
$1s\,2s\,4s(^4S)$		671.6	667.9	-2.8 $+2.9$	10
$1s\,2s\,4s(^2S_-)$		672.9	672.0	-1.1 $+1.2$	11
$1s\,2s\,4p(^4P)$		673.2			12
$1s\,2s\,4p(^2P_-)$		673.5			13
$1s\,2s\,5s(^4S)$		688.4	682.5	-1.3 $+2.4$	14
$1s\,2s\,5s(^2S_-)$		689.0			15
$1s\,2s\,5p(^4P)$		689.2			16
$1s\,2s\,5p(^2P_-)$		689.5			17
$1s\,2s\,6s(^4S)$		697.2	691.6	-2.3 $+2.7$	18
$1s\,2s\,6s(^2S_-)$		697.5			19
$1s\,2s\,6p(^4P)$		697.7			20
$1s\,2s\,6p(^2P_-)$		697.9			21

[a]Chung (Ref. 27).
[b]Bhalla (Refs. 28).

the target area, while approximately 1% of the F^{7+} $(1s\,2s)\,^1S$ metastable state created at the post-stripping foil reaches the target area. The fraction of the total F^{7+} beam which is in the $(1s\,2s)\,^3S$ metastable state at the target chamber was measured as a function of beam energy and was found to be between 9% and 25%.[5] These fractions are necessary to determine the cross sections for projectile events involving the $(1s\,2s)\,^3S$ metastable state of fluorine. Schiebel *et al.*[25] have reported a variation in the fraction of the metastable component as a function of foil thickness. However, a survey of the available literature relevant to this problem indicates that the variation in the metastable fraction between gases and thin foils is approximately 25% (Ref. 26) which is on the order of the errors reported in Ref. 5. The fraction of the total F^{7+} beam which is in the $(1s\,2s)\,^1S$ state will be negligible compared to the $(1s\,2s)\,^3S$ metastable-state fraction.

Since the $(1s\,2s)\,^3S$ metastable state of the fluorine projectile has an initial K-vacancy, single-electron capture to an excited state of the projectile can result in a K-Auger transition, whereas the two-electron ground state of the projectile must undergo a double process (i.e., simultaneous K-shell excitation and single capture to an excited state) to produce a K-Auger transition. The double process is much less probable than the process of single-electron capture and thus the F^{7+} spectra in Fig. 1 are attributed, predominantly, to single-electron capture to excited states of the $(1s\,2s)\,^3S$ metastable component of the two-electron fluorine beam and the subsequent K-Auger decay of the three-electron states thus created.

The theoretical K-Auger decay energies of the three-electron states are shown in Fig. 1 compared to the spectra for 6-MeV $F^{7+}+He$ and 6-MeV $F^{7+}+Ne$ in the projectile rest frame. The theoretical energies and the experimental rest-frame energies of the major peaks are tabulated for comparison in Table II. The column marked "label" in Table II corresponds to the the position numbers in Fig. 1 for identification purposes. The upper calculations in Fig. 1 are those of Chung,[27] and the lower calculations from Bhalla *et al.*[28,29] Both sets of calculations were normalized to the projectile rest-frame energy of the second major peak for $F^{7+}+He$ in Fig. 1. As can be seen from Fig. 1, both the spectral peaks and the calculations are in definite groupings corresponding to electron capture to a specific shell or level of the F^{7+} $(1s\,2s)\,^3S$ metastable state. Thus the lowest-energy group in Fig. 1 corresponds to electron capture to the $n=2$ level of fluorine, the next group corresponds to electron capture to the $n=3$ level of fluorine, etc., all the way out to the series limit. The groupings of the calculations correspond very well with

the peak groupings and reinforce the above identification of the peak groupings.

The resolution of the analyzer was not sufficient to conduct a positive identification of the individual states within each grouping, especially for the higher-n values. As can be seen from Table II, there are four individual states that may be present for $n=2$, while only two major peaks for helium are experimentally distinguished. The $(1s\,2s^2)\,^2S$, the $(1s\,2s\,2p)\,^4P$, and the $(1s\,2s\,2p)\,^2P_-$ are all assumed to be formed from the F^{7+} $(1s\,2s)\,^3S$ component of the beam, and the $(1s\,2s\,2p)\,^2P_+$, included for completeness, is formed from the $(1s\,2s)\,^1S$ state of F^{7+}. Throughout Table II the minus and plus subscripts indicate lower- and higher-energy multiplets formed from the F^{7+} $(1s\,2s)\,^3S$ state and the F^{7+} $(1s\,2s)\,^1S$ state, respectively.

The neon spectrum in Fig. 1 has noticeably more structure on the high-energy side of each grouping than exhibited in the helium spectrum. The added structure is thought to be due to *multiple-capture* events where the additional captured electrons act as "spectator" electrons participating in the Auger transition only by screening the nuclear charge of the projectile. The K-Auger decay energies of the $1s\,2s^2 2p^k$ and the $1s2s2p^m$ states have been calculated by Can *et al.*[28] and found to lie between 535 and 600 eV. These configurations correspond to multiple capture to the $n=2$ level of the $(1s\,2s)\,^3S$ metastable state of fluorine. For the case of fluorine incident on a neon target (see Fig. 1), the added structure observed at the higher

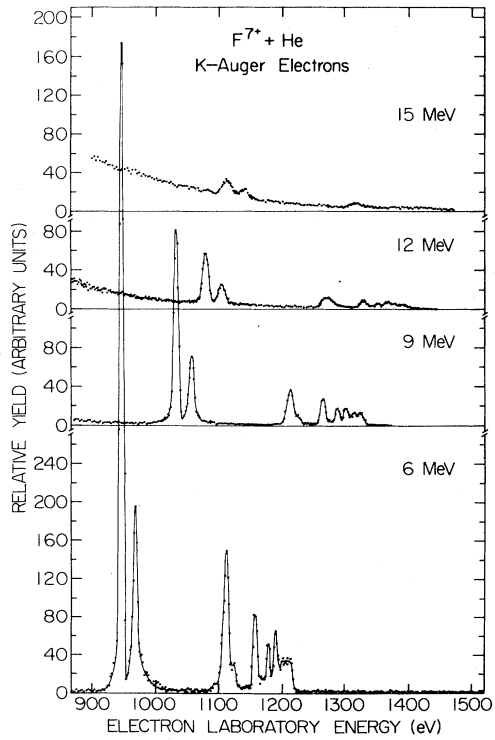

FIG. 2. Energy dependence of $F^{7+}+He$ spectra illustrating the kinematic energy shift of the peaks, the kinematic broadening effects, and the δ-electron background present in all the spectra taken.

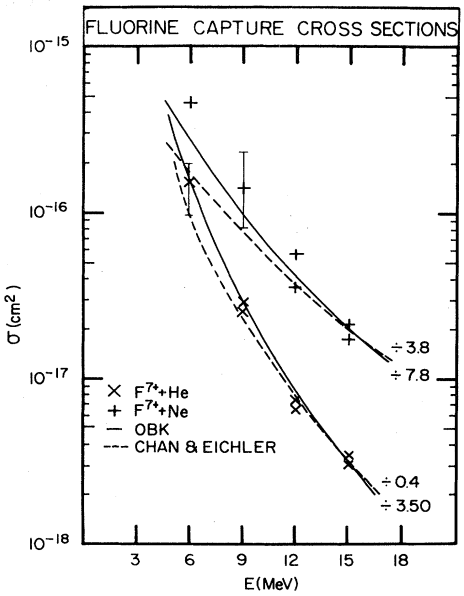

FIG. 3. Energy dependence of the fluorine-capture cross sections for $F^{7+}+He$ and $F^{7+}+Ne$ compared to an OBK calculation (Ref. 31) and an eikonal approach to electron capture (Chan and Eichler) (Refs. 32 and 33). Both calculations are normalized to the corresponding 15-MeV data points.

energies for $n=2$ falls within the range of the calculated multiple-capture states. For the case of a helium target, the only possible multiple-capture event is double capture which is an order of magnitude smaller than single capture for fluorine on helium or double capture for fluorine on neon.[15,30]

The energy dependence of the F^{7+} + He spectra in the laboratory frame is shown in Fig. 2 and is representative of the energy dependence for the F^{7+} + Ne spectra. Figure 2 also illustrates the energy dependence of the δ electron background. As is expected and shown in Fig. 2, the more violent the collision (i.e., the higher the incident energy) the more δ electrons are produced. Also depicted in Fig. 2 are the kinematic broadening effects and the kinematic shift in energy of electrons ejected from a moving emitter described by Eq. (3.4).

The energy dependence of the cross sections for electron capture to excited states of fluorine are compared to an Oppenheimer-Brinkman-Kramers[31] (OBK) approximation for electron capture and to an eikonal approach to electron capture (Chan and Eichler)[32,33] in Fig. 3. It is well known[34,35] that the OBK approximation considerably overestimates the experimental total cross section but otherwise reflects the correct behavior at high velocities. With an eikonal approach, Chan and Eichler[32,33] obtain the cross section for electron capture in terms of the corresponding OBK cross section and a scaling term. The calculations were independently normalized to the 15-MeV data for both targets with larger normalization factors for the OBK calculation as expected. As can be seen in Fig. 3, both calculations appear to be in good agreement with the energy dependence of the data for both targets although the OBK appears to be in slightly better agree-

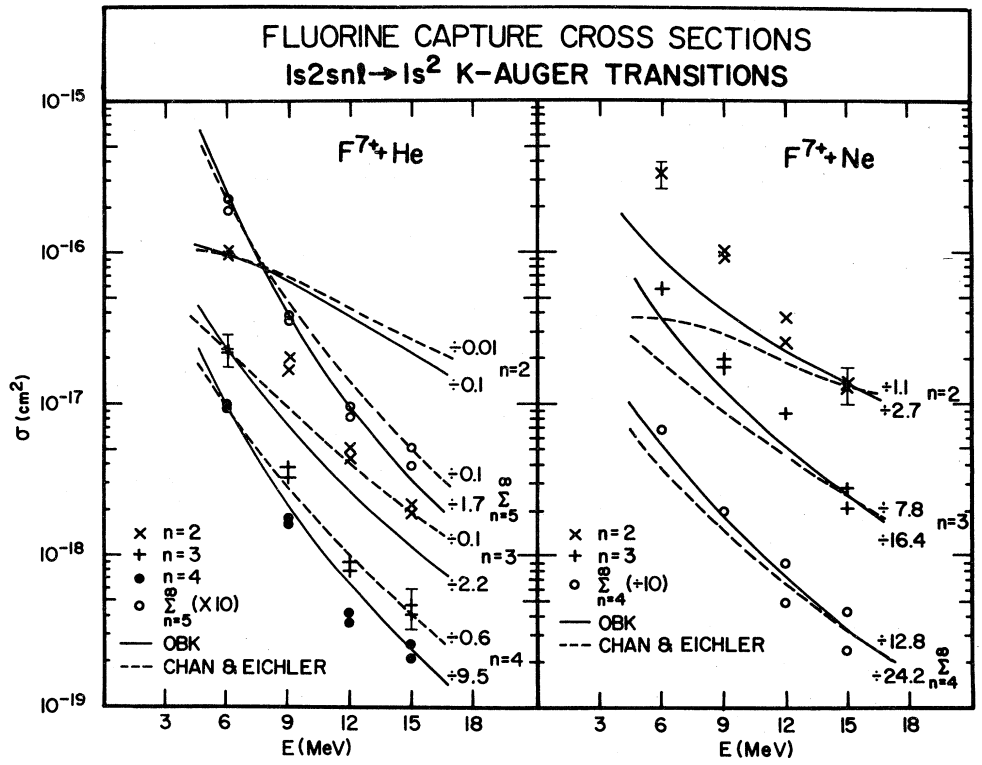

FIG. 4. Energy dependence of the fluorine partial-capture cross sections for helium and neon gas targets. $\sum_{n=5}^{\infty}$ indicates the partial cross section including all higher values of n. The cross sections are compared to the OBK (Ref. 31) and the Chan and Eichler (Refs. 32 and 33) calculations.

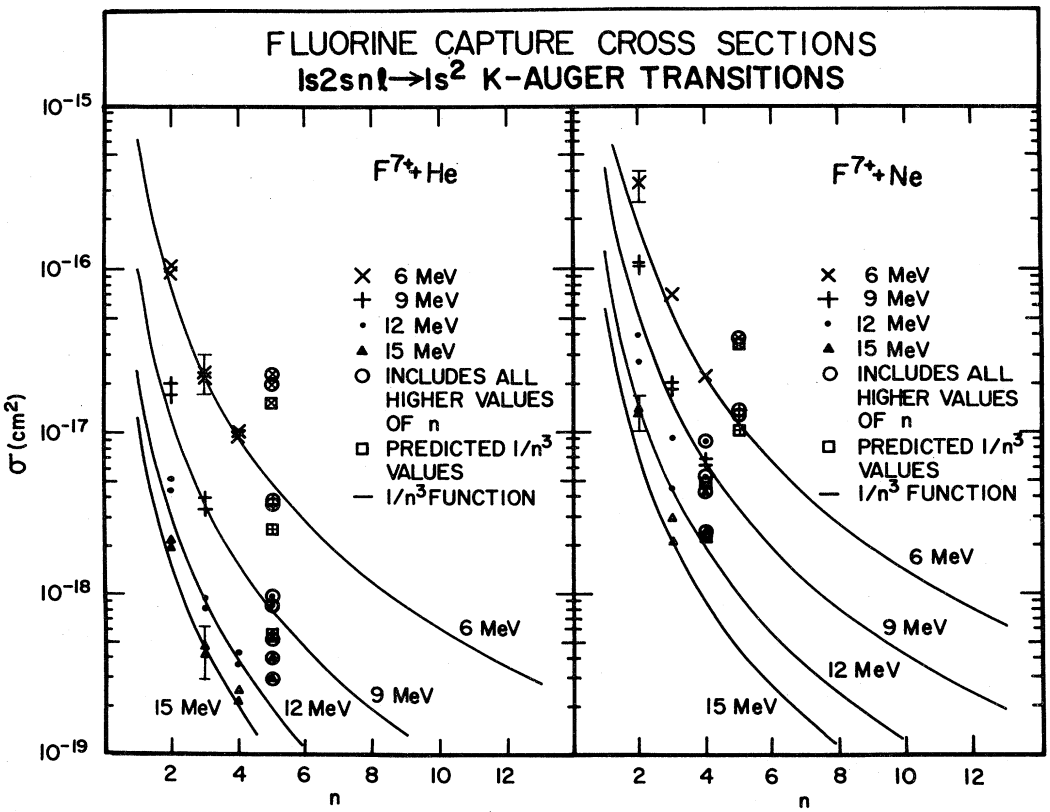

FIG. 5. n dependence of the fluorine partial-capture cross sections for $F^{7+}+He$ and $F^{7+}+Ne$ compared to a $1/n^3$ function.

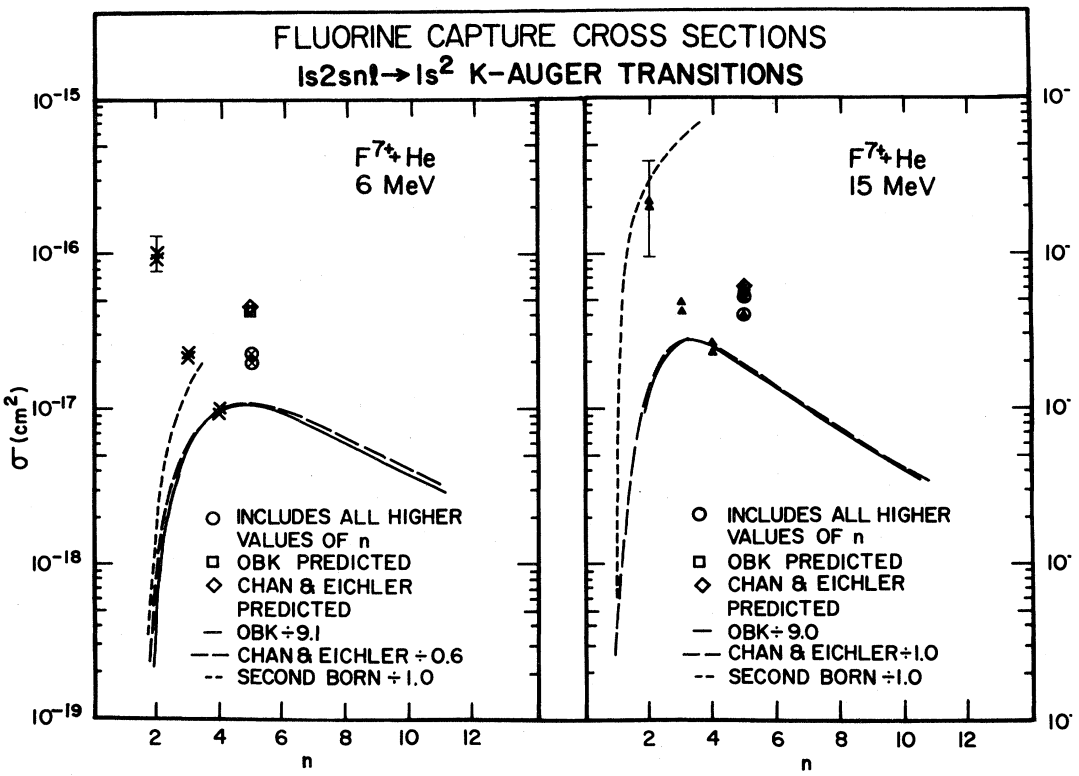

FIG. 6. n dependence of the fluorine partial-capture cross sections for 6-MeV $F^{7+}+He$ (indicated by $\times$) and 15-MeV $F^{7+}+He$ (indicated by ▲) compared to the predicted n distribution of the OBK approximation (Ref. 31), the Chan and Eichler calculation (Refs. 32 and 33), and a second Born calculation (Refs. 36—38).

ment. It should be noted that, since the spectra and thus the cross sections presented in this section result from the incident F^{7+} $(1s\,2s)\,^3S$ metastable state, the cross sections have been adjusted by the energy-dependent fraction of the $(1s\,2s)\,^3S$ metastable component of the beam which survives to the target area.[5]

From Fig. 1, it is evident that not only can the total cross section be obtained, but also the partial cross sections for $n=2$, 3, and 4 and the partial cross section for the sum of all higher n ($\sum_{n=5}^{\infty}$ in the following figures). The energy dependence of the partial cross sections is displayed in Fig. 4 and compared to the previously mentioned calculations for the corresponding n level. For the helium case the calculations, which are normalized to the 6-MeV data points, and the data tend toward better agreement as the value of n increases. The $n=2$ partial cross sections ($\times$'s) and the calculations are in poor agreement while the partial cross sections for $\sum_{n=5}^{\infty}$ (○'s) are in excellent agreement. For the neon case the agreement between the calculations, normalized to the 15-MeV data points, and the cross sections follow the same trend as in the helium case. Overall, the normalization constants for the neon data are greater than the normalization constants for the helium data in both Figs. 3 and 4. This perhaps reflects the problems inherent in using perturbation calculations for near-symmetric collisional systems, particularly at low velocities.

According to the OBK approximation,[31] electron capture to excited states should follow a $1/n^3$ dependence for

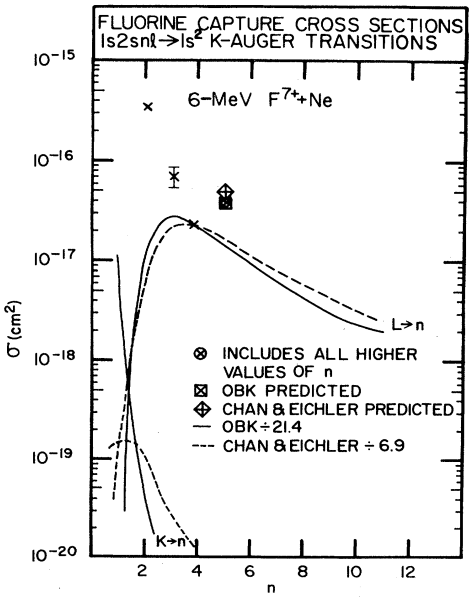

FIG. 7. n dependence of the fluorine partial-capture cross sections for 6-MeV $F^{7+}+Ne$ compared to the OBK (Ref. 31) and the Chan and Eichler (Refs. 32 and 33) calculations. $K\rightarrow n$ ($L\rightarrow n$) refers to the calculated values for capture of a neon K-shell (L-shell) electron into an excited state of fluorine.

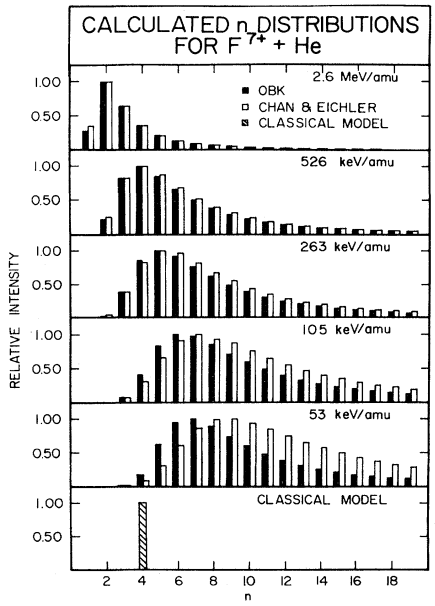

FIG. 8. Energy dependence of the calculated n distributions for $F^{7+}+He$.

sufficiently large velocities or sufficently high n levels. Figure 5 shows the n dependence of the fluorine partial-capture cross sections compared to a $1/n^3$ function for each target gas at each incident-projectile energy. The circled data points represent the sums of the partial cross sections for all states with $n \geq 5$ and the squared data points represent the corresponding $1/n^3$ function predictions. It is evident from Fig. 5 that the partial cross sections do indeed follow a $1/n^3$ function.

Figure 6 presents the partial cross sections for two energies of fluorine on a helium target compared to the corresponding OBK, Chan and Eichler, and second Born calculations.[36,37] It is obvious from Fig. 6 that, although the experimental partial cross sections might exhibit a $1/n^3$ dependence, neither the OBK nor the Chan and Eichler calculation is at sufficiently high velocities to vary as $1/n^3$. Therefore, either the calculations do not predict the correct n dependence, or some process not presently considered is affecting the data, or possibly a combination of both. Included for comparison is a second Born calculation[38] for $n=1$, 2, and 3 even though the second Born is not expected to be valid at the velocities considered. Indeed, the second Born is in no better agreement with the experimental n distributions than the other two calculations.

The n dependence of the partial cross sections for 6-MeV $F^{7+}+Ne$ is compared, in Fig. 7, to the OBK calculation and to the Chan and Eichler calculation for electron capture from the L shell of neon to an excited state of fluorine and for electron capture from the K shell of neon to an excited state of fluorine. Again, good agreement between the data and the calculations is not evident. In addition to the difference in normalization between the OBK and the Chan and Eichler calculations, the two theories predict quite different $K \rightarrow n$ partial-capture cross sections.

The energy dependence of the relative predicted n distributions for $F^{7+}+He$ are illustrated in Fig. 8 for both the OBK and the Chan and Eichler calculations. Also shown in Fig. 8 is the most probable n value of the final state occupied by the captured electrons calculated with a classical treatment for low-energy collisions ($E \leq 10$ keV/amu).[39] It is interesting to note that the quantum-mechanical treatments, in the low-velocity limit, do not approach the n value predicted by the classical treatment, but at the high velocities, do approach the experimental n distributions for $F^{7+}+He$ (cf. Fig. 6).

The relative experimental fluorine n distributions (or n populations), calculated from the partial-capture cross sections in Fig. 5 and normalized to the total cross section for the corresponding projectile energy, are tabulated for helium and neon in Tables III and IV, respectively. Also listed are the n populations calculated from the relative-projectile x-ray intensities measured by Hopkins *et al.*[40] The n populations calculated from both the x-ray measurements and the Auger measurements agree very well with each other and vary only slightly with incident-projectile energy. The relative fluorine populations for both targets vary as $1/n^3$ for $n \geq 3$. For $n=2$, the popu-

TABLE III. Relative n populations for fluorine projectiles incident on helium.

	$n=2$	$n=3$	$n=4$	$n=5$	$\sum_{n=4}^{\infty}$	$\sum_{n=5}^{\infty}$
6 MeV	0.66	0.15	0.07			0.13
	0.64	0.15	0.06			0.05
9 MeV	0.68	0.13	0.06			0.13
	0.66	0.13	0.06			0.14
12 MeV	0.69	0.13	0.06			0.13
	0.69	0.13	0.06			0.13
15 MeV	0.66	0.14	0.07			0.13
	0.63	0.14	0.08			0.15
35.6 MeV[a]	0.60	0.20	0.10	0.10		
	0.67	0.33				
Average	0.66	0.14	0.07			0.13

[a]Taken from the x-ray measurements of Hopkins *et al.* (Ref. 40).

TABLE IV. Relative n populations for fluorine projectiles incident on neon.

	$n=2$	$n=3$	$n=4$	$n=5$	$\sum_{n=4}^{\infty}$	$\sum_{n=5}^{\infty}$
6 MeV	0.72	0.15	0.05		0.13	0.08
9 MeV	0.74	0.13	0.05		0.13	0.09
	0.71	0.15	0.04		0.14	0.10
12 MeV	0.69	0.16			0.15	
	0.73	0.12			0.14	
15 MeV	0.66	0.13			0.21	
	0.74	0.12			0.14	
35.6 MeV[a]	0.68	0.20	0.08	0.05		
	0.73	0.17	0.09			
Average	0.71	0.15	0.06		0.15	0.09

[a]Taken from the x-ray measurements of Hopkins *et al.* (Ref. 40).

lations are larger than expected from the $1/n^3$ function.

It was mentioned earlier that there might exist processes or effects not accounted for in the partial-capture cross sections that would lead to the large disagreement between the data and the theories. One factor that has been ignored so far is the lifetimes of the states created after electron capture. If the lifetimes of these states are comparable to or longer than the time the projectile spends in the viewing region of the analyzer, the actual total intensities for these states will be larger than the observed intensities. An expression for the ratio of the observed intensity to the total intensity is given by[40]

$$R=\int_{x_0}^{x_0+x_1}\frac{(1-e^{-\lambda X})dX}{X_1}\ , \tag{4.1}$$

where X_0 is the distance from the entrance aperture of the gas cell to the start of the viewing region of the analyzer, X_1 is the length of the viewing region, and λ is a decay constant. The decay constant is expressed in units of inverse length and is given by

$$\lambda=\frac{1}{v\tau}\ , \tag{4.2}$$

where v is the projectile velocity and τ is the lifetime of the state of interest. Most of the states created by electron capture to the fluorine projectile have relatively short lifetimes ($\sim 10^{-4}-10^{-15}$ sec),[19] but the F^{7+} $(1s\,2s\,2p)\,^4P$ states have much longer lifetimes ($\sim 2-16\times 10^{-9}$ sec).[41,42] Thus for the projectile energies studied in the present work, the majority (70–85 %) of the contribution of the $(1s\,2s\,2p)\,^4P_{3/2,1/2}$ states is observed, but less than 20% of the $(1s\,2s\,2p)\,^4P_{5/2}$ contribution is observed. The difficulties in correcting the partial-capture cross sections for $n=2$ all relate to instrument resolution. First, the $(1s\,2s\,2p)\,^4P$ multiplet cannot be separated from the $(1s\,2s^2)\,^2S$ multiplet with the spectrometer in the present configuration so that the contribution of the $(1s\,2s\,2p)\,^4P$ to the partial-capture cross section for $n=2$ cannot be determined. Second, the contributions of the various states to the $(1s\,2s\,2p)\,^4P$ multiplet intensity cannot be directly determined, although they can be estimated statistically. Even if the lifetime corrections for these metastable states, which apply to the total-capture cross sections as well as the partial-capture cross sections for $n=2$, were easily applicable, the effect on the partial-capture cross sections for $n=2$ would be to raise the cross section. This would give worse agreement with the theory (cf. Fig. 6).

Cascading via x-ray transitions is another possible factor which can alter the observed n distributions. It would

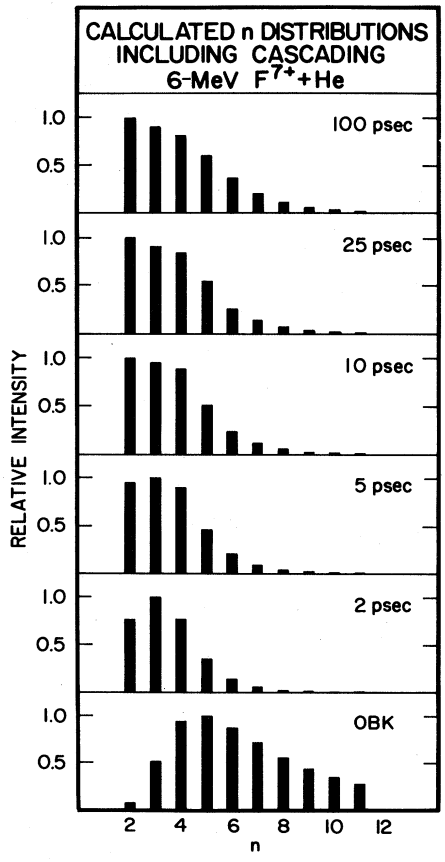

FIG. 9. Predicted n distributions of 6-MeV F^{7+}+He as a function of time using an OBK calculation with cascading effects included.

TABLE V. Predicted and observed ($1s\,2snl$) K-Auger relative yields.

n	OBK No cascading	OBK With cascading	Measured
2	1.00	1.00	1.00
3	9.71	0.91	0.23
4	18.02	0.81	0.10
$\sum_{n=5}^{\infty}$	80.81	1.39	0.14

raise the observed K-Auger cross sections for the smaller values of n, and, if included in the calculations, it would elevate the predicted intensities for the smaller values of n. Figure 9 illustrates the effects of cascading after different time intervals on the n distribution of the initial OBK calculation for 6-MeV $F^{7+}+He$. The cascading model[43–45] used for the calculation utilizes a hydrogenlike model for the necessary transition probabilities and assumes that only $E1$ x-ray transitions are possible channels for cascading. Nevertheless, as more time is allowed for cascading events to occur, the calculated n distribution approaches the trend of the experimental n distribution (cf. Fig. 6).

The n distribution stabilizes after about 25 psec, which is much shorter than the 380-psec total viewing time of the analyzer for 6-MeV F^{7+} ions. The OBK-predicted n distributions, including cascading, give better agreement with the measured K-Auger yield than the OBK without cascading, as can be seen in Table V. Nevertheless, the agreement is not very good and the conclusion is that the OBK and the Chan and Eichler calculations are predicting n distributions at low-ion velocities that are peaked at higher-n values than is found experimentally.

V. CONCLUSION

The projectile K-Auger electron-production cross sections resulting from electron capture to excited states of the two-electron $(1s\,2s)\,^3S$ metastable ion of fluorine are reported. The K-Auger emission spectra of the resulting ($1s\,2snl$) three-electron states are measured with sufficiently high resolution to distinguish electron capture to several of the low-lying n values. The corresponding F K-Auger electron-production cross sections are reported as a function of the n level into which the electron is captured. The data for these n distributions agree with a $1/n^3$ function, although perhaps fortuitously, since lifetime and x-ray cascading effects are present in the data. The effects of cascading, via $n \rightarrow n'$ $(n > n' \geq 2)$ $E1$ x-ray transitions, on the OBK-calculated n distributions for electron capture are presented. Without the effects of x-ray cascading, the OBK calculation for low-ion velocities predicts a maxima in the n distribution at high values of n $(n \sim 7)$ and does not converge to the value of n $(n=4)$ predicted by a classical model.[39] With the effects of x-ray cascading, the agreement for low-ion velocities between the OBK-calculated n distribution and the experimentally determined n distribution is better but still not very good. It is concluded that the experimental n distribution peaks at a lower value of n than predicted by theory for energies near 6 MeV.

ACKNOWLEDGMENT

This work was supported by the U.S. Department of Energy, Division of Chemical Sciences.

*Permanent address: University of South Alabama, Mobile, Alabama

†Permanent address: Oak Ridge National Laboratory, Oak Ridge, Tennessee

[1]N. Stolterfoht, D. Schneider, D. Burch, B. Aagaard, E. Børing, and B. Fastrup, Phys. Rev. A 12, 1313 (1975).

[2]C. W. Woods, Robert L. Kauffman, K. A. Jamison, N. Stolterfoht, and Patrick Richard, J. Phys. B 8, L61 (1975).

[3]D. Schneider, R. Bruch, W. Butscher, and W. H. E. Schwarz, Phys. Rev. A 24, 1223 (1981).

[4]Philip L. Pepmiller and Patrick Richard, Phys. Rev. A 26, 786 (1982).

[5]M. Terasawa, Tom J. Gray, S. Hagmann, J. Hall, J. Newcomb, P. Pepmiller, and Patrick Richard, Phys. Rev. A 27, 2868 (1983).

[6]M. D. Brown, L. D. Ellsworth, J. A. Guffey, T. Chiao, E. W. Pettus, L. M. Winters, and J. R. Macdonald, Phys. Rev. A 10, 1255 (1974).

[7]R. Bruch, L. J. Dubé, E. Trübert, P. H. Heckman, B. Raith, and K. Brand, J. Phys. B 15 L857 (1982).

[8]P. Hvelplund, E. Samsøe, L. H. Anderson, H. K. Haugen, and H. Knudsen, Phys. Scr. T3, 176 (1983).

[9]H. Knudsen, P. Hvelplund, L. H. Anderson, S. Bjørnelund, M. Frost, H. K. Haugen, and E. Samsøe, Phys. Scr. T3, 101 (1983).

[10]Yu. S. Gordeev, D. Dijkkamp, A. G. Drentje, and F. J. de Heer, Phys. Rev. Lett. 50, 1842 (1983).

[11]C. L. Cocke, R. DuBois, T. J. Gray, E. Justiniano, and C. Can, Phys. Rev. Lett. 46, 1671 (1981).

[12]R. Mann, F. Folkman, and H. F. Beger, J. Phys. B 14, 1161 (1981); R. Mann, C. L. Cocke, A. Schlachter, M. Prior, and R. Marrus, Phys. Rev. Lett. 18, 1329 (1982).

[13]S. Ohtani, Y. Kaneko, M. Kimura, N. Kobayashi, T. Iwai, A. Matsumato, K. Okuno, S. Takagi, H. Tawara, and S. Tsurubuchi, J. Phys. B 15, L535 (1982).

[14]H. Tawara, M. Terasawa, Patrick Richard, Tom J. Gray, P. Pepmiller, J. Hall, and J. Newcomb, Phys. Rev. A 20, 2340 (1979).

[15]H. Tawara, Patrick Richard, K. A. Jamison, Tom J. Gray, J. Newcomb, and C. Schmiedekamp, Phys. Rev. A 19, 1960 (1979).

[16]C. W. Woods, Robert L. Kauffman, K. A. Jamison, C. L. Cocke, and Patrick Richard, J. Phys. B 7, L474 (1974); C. W. Woods, R. L. Kauffman, K. A. Jamison, N. Stolterfoht, and P. Richard, Phys. Rev. A 13, 1358 (1976).

[17]L. H. Toburen, Phys. Rev. A 3, 216 (1971).

[18]H. Becker, E. Dietz, and U. Gerhardt, Rev. Sci. Instrum. 43, 1587 (1972).

[19]T. W. Tunnell, C. Can, and C.P. Bhalla, IEEE Trans. Nucl. Sci. 26, 1124 (1979).

[20]The analyzer was designed by Mr. Erick Feldl with the assistance of Dr. C. L. Cocke and Dr. M. D. Brown, all from

Kansas State University at the time, using the parameters given in Ref. 21. The analyzer was constructed in the precision machine shop at Kansas State University.
[21]J. S. Risley, Rev. Sci. Instrum. 43, 95 (1972).
[22]Joal J. Newcomb, Ph.D. thesis, Kansas State University, 1983.
[23]Clifford Warren Woods, Ph.D. thesis, Kansas State University, 1975.
[24]T. R. Dillingham, M. S. thesis, Kansas State University 1980.
[25]U. Schiebel, B. L. Doyle, J. R. Macdonald, and L. D. Ellsworth, Phys. Rev. A 16, 1089 (1977).
[26]T. R. Dillingham, Ph.D. thesis, Kansas State University 1983.
[27]K. T. Chung (private communication).
[28]C. P. Bhalla (private communication); C. Can, T. W. Tunnell, and C. P. Bhalla, J. Electron Spectrosc. Relat. Phenom. 27, 75 (1982).
[29]T. W. Tunnell (private communication).
[30]Patrick Richard, Philip L. Pepmiller, and K. Kawatsura, Phys. Rev. A 25, 1937 (1982).
[31]M. R. C. McDowell and J. P. Coleman, *Introduction to the Theory of Ion-Atom Collisions* (North-Holland, Amsterdam, 1970), Sec. 8.2.
[32]Jörg Eichler and F. T. Chan, Phys. Rev A 20, 104 (1979).
[33]F. T. Chan and Jörg Eichler, Phys. Rev. A 20, 1841 (1979).
[34]V. S. Nikolaev, Zh. Eksp. Teor. Fiz. 51, 1263 (1966) [Sov. Phys. JETP 24, 847 (1967)].
[35]A. M. Halpern and J. Law, Phys. Rev. Lett. 31, 4 (1973).
[36]J. S. Briggs and L. Dubé, J. Phys. B 13, 771 (1980).
[37]Louis J. Dubé and John S. Briggs, J. Phys. B 14, 4594 (1981).
[38]Calculations courtesy of J. H. McGuire (private communication).
[39]Hirashi Ryutuku, Ken Sasaki, and Tsutomi Watanabe, Phys. Rev. A 21, 745 (1980).
[40]Forrest Hopkins, Robert L. Kauffman, C. W. Woods, and Patrick Richard, Phys. Rev. A 9, 2413 (1974).
[41]C. P. Bhalla and T. W. Tunnell, Z. Phys. A 303, 199 (1981).
[42]P. Richard, R. L. Kauffman, F. F. Hopkins, C. W. Woods, and K. A. Jamison, Phys. Rev. A 8, 2187 (1973).
[43]L. J. Curtis, Am. J. Phys. 36, 1123 (1968).
[44]L. J. Curtis, J. Opt. Soc. Am. 64, 495 (1974).
[45]Richard M. Schectman, Phys. Rev. A 12, 1717 (1975).